

Modulating Spin Delocalization in Phenoxy Radicals Conjugated with Heterocycles

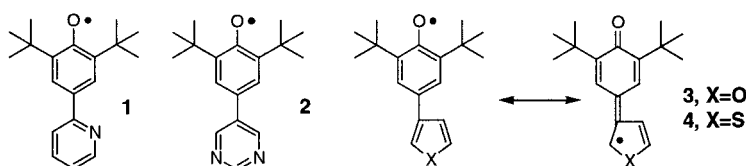
Chunping Xie,[†] Paul M. Lahti,^{*,†} and Clifford George[‡]

Department of Chemistry, University of Massachusetts, Amherst, Massachusetts 01003,
and Laboratory for the Structure of Matter, Naval Research Laboratory,
Washington, D.C. 20375

lahti@chem.umass.edu

Received July 17, 2000

ABSTRACT



Phenoxy radicals were synthesized having heterocyclic substituents in the 4-position. Electron spin resonance spectroscopy shows spin density can be modulated by delocalization onto the heterocycle structure, to the extent that some of the largest spin density bearing sites in 3 and 4 lies in the heterocycle, not in the phenoxy ring.

Sterically stabilized phenoxy radicals have been known for almost a half-century as subjects of electron spin resonance (ESR), UV-vis, and infrared studies. 2,6-Di-*tert*-butylphenoxy radicals are persistent in deoxygenated solution, but generally dimerize and decompose in the solid state, with the exception of the structurally related galvinoxyl radical.¹ Infrared and ESR spin density studies show stabilized phenoxy radicals to be highly delocalized, with considerable C=O character. Recent efforts to design organic-based molecular magnetic materials have impelled studies of electronic structure in delocalized open-shell organic molecules.² In this report, we describe the generation of 2,6-di-*tert*-butylphenoxy radicals **1**–**4** with conjugated heterocyclic rings attached at the 4-position and show spectroscopically that delocalization varies considerably as a function of the heterocycle structure and is so extensive in some cases that

major spin density bearing sites are found beyond the phenoxy radical moiety.

Scheme 1 shows the syntheses of the phenol precursors **5**–**8**. In each case the key step is the palladium-catalyzed Suzuki coupling of trimethylsilyl-protected 2,6-di-*tert*-butylphenol-4-boronic acid³ **9** with the appropriate heteroarene. Deprotection occurs during workup, directly yielding the phenols after column chromatography. Spectral and elemental characterizations of all new compounds were satisfactory. The characteristically narrow OH band of a 2,6-di-*tert*-butylphenol was observed in the FTIR spectrum for KBr-pelletized solid samples of **5**, **7**, and **8**. Curiously, a broadened OH band was observed for **6** under the same conditions, suggesting the presence of hydrogen bonding, despite the steric blockading due to the *tert*-butyl groups. X-ray crystallographic analysis⁴ confirmed the presence of hydrogen bonding between the phenolic OH and the pyrimidine nitrogen of another molecule in the crystal lattice. Figure 1 shows a schematic diagram of this hydrogen

[†] University of Massachusetts.

[‡] Naval Research Laboratory.

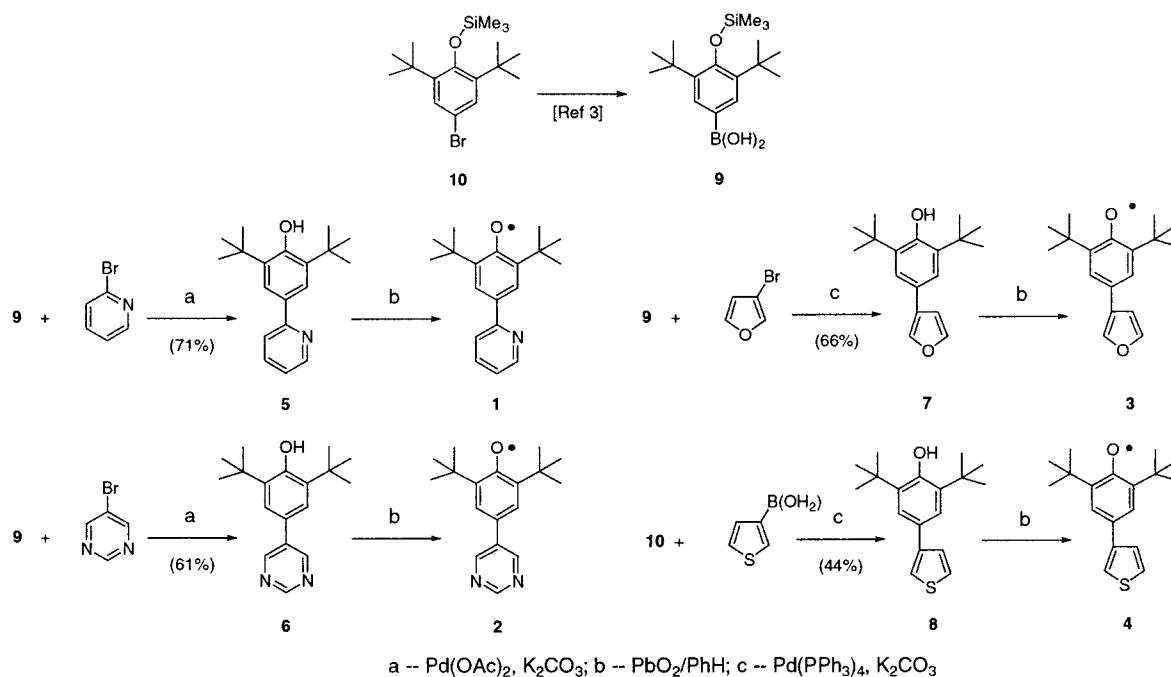
(1) Altwicker, E. R. *Chem. Rev.* **1967**, *67*, 475.

(2) (a) Kahn, O. *Molecular Magnetism*; VCH: New York, 1993. (b) Turnbull, M. M.; Sugimoto, T.; Thompson, L. K., Eds. *Molecule-based Magnetic Materials. Theory, Techniques, and Applications*; American Chemical Society, Washington, DC, 1996; Vol. 644. (c) Lahti, P. M., Ed. *Molecular Magnetism in Organic-Based Materials*; Marcel Dekker: New York, 1999.

(3) Satoh, Y., Shi, C. *Synthesis* **1994**, 1146.

(4) Selected crystallographic data for **6**: orthorhombic, *Pna*2₁; orthorhombic (*Z* = 4), *a* = 12.118(1), *b* = 7.514(1), *c* = 18.799(2) Å. Selected lengths, angles, torsions: O1–N5A = 2.797(3) Å, H–N5A = 2.24(4) Å, O1–H–N5A = 123(3)°, C2'–C1'–C3–C4 = 35.1°, C2–C1–O1–H = 27.1°.

Scheme 1



bonding arrangement in **6**. Additional data is given in the Supporting Information. Further support for the presence of this somewhat surprising hydrogen bonding motif is given by the fact that a 1:1 coordination complex between **6** and copper(II) chloride shows the return of a typical, narrow OH band at 3620 cm⁻¹ in the FTIR, presumably because the nitrogen acceptor sites are now at least partly coordinated by copper.

The phenols were oxidized in degassed benzene by stirring with lead dioxide recently prepared by hydrolysis of lead tetraacetate. The solutions rapidly became colored, as is characteristic for formation of phenoxyl radicals. The longest wavelength UV-vis bands of **1–4** were 496, 614, 420, and

698 nm, respectively. Extinction coefficients and radical concentrations were not determined due to the instability of **1–4** over extended time periods. Radical **3** showed no longer

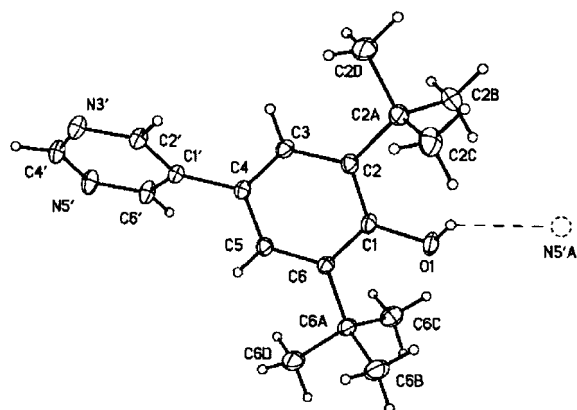


Figure 1. Hydrogen bonding in phenol **6**, taken from a single-crystal X-ray analysis. N5'A is symmetry generated. See Supporting Information for further structural details.

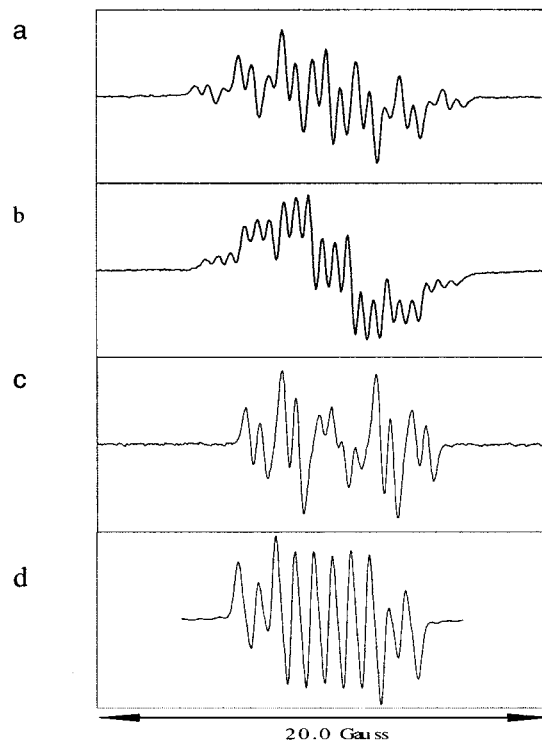
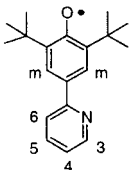
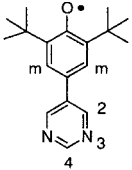
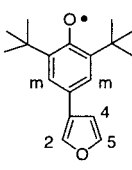
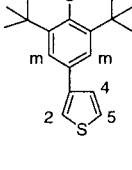


Figure 2. Room-temperature ESR spectra of **1** (curve a, 9.791 GHz), **2** (curve b, 9.791 GHz), **3** (curve c, 9.800 GHz), **4** (curve d, 9.798 GHz).

range band in the >500 nm range, but has a long absorbance tail that makes it appear yellow in dilute solution but red at higher concentrations.

Figure 2, curves a–d, show the X-band ESR spectra of the radical solutions. The hyperfine coupling constants (hfc) were obtained by line shape analysis of the spectra using the WINSIM program of Duling.⁵ To assist with the hfc assignments, density functional computations were carried out using Gaussian 98⁶ at the BLYP/cc-pVDZ level, using B3LYP/6-31G* optimized geometries for model systems where the *tert*-butyl groups were replaced by hydrogen atoms. All computed geometries gave essentially coplanar rings. All computed hfc were taken directly from the Gaussian computations, which are based upon the computed Fermi contact couplings. Table 1 summarizes the experi-

Table 1. Experimental and Computed hfc for 1–4

Radical	Expt hfc ^a	Computed hfc ^b
	a(m) = 1.8 G a(N) = 1.4 G a(3,5) = 0.5–0.6 G a(4,6) = 1.9–2.1 G	[a(m) = -1.1 G] a(N) = -1.0 G a(3,5) = -0.3, -0.4 G a(4,6) = 1.7, 2.0 G
	a(m) = 1.8 G a(N) = 0.5 G a(2) = 1.6 G a(4) = 1.8 G	[a(m) = -1.1 G] a(N) = -0.3 G a(2) = 1.2 G a(4) = 1.5 G
	a(m) = 1.6 G a(2) = 4.2 G a(4) = 0.6 G a(5) = 0.2 G	[a(m) = -0.9 G] a(2) = 3.8 G a(4) = 0.4 G a(5) = 0.2 G
	a(m) = 1.6 G a(2) = 3.3 G a(4) = 0.8 G a(5) = 0.3 G	[a(m) = -1.4 G] a(2) = 3.8 G a(4) = 0.8 G a(5) = -0.2 G

^a Hfc are absolute values based on WINSIM simulations. ^b Signs are based on expected negative hfc for a(m), for model systems with *tert*-butyl groups replaced by hydrogen, computed at the BLYP/cc-pVDZ//B3LYP/6-31G* level.

mental hfc for 1–4 and the computed hfc for the model systems. The brackets around a(m) emphasize that these computed hfc are likely to be influenced by the replacement of the *tert*-butyl groups, relative to the actual experimental values.

The solution ESR spectra and colors of 1–4 persisted for up to 3 days under nitrogen, but faded swiftly when exposed to air. When solvent was removed, the resultant solids lightened in color upon exposure to air: the color change is irreversible and the radicals nonrecoverable. The persistence

of these systems appears to be somewhat lower than that of the 4-(1*H*-benzimidazol-2-yl)-2,6-di-*tert*-butylphenoxy systems that we have described previously.⁷ For example, system 2 shows the appearance of bands in the C=O region of the FTIR in KBr pellets, implying considerable dimerization. Systems 3 and 4 appear not to dimerize so readily and also show longer-lived coloration in solution upon exposure to air.

ESR hyperfine analysis shows the extent of delocalization of the unpaired spin from the phenoxy radical moiety. In systems 3 and 4, the largest hydrogen hyperfine coupling constant is found on the heterocyclic ring system, not on the phenoxy unit. This demonstrates the extent to which the spin density in a conjugated radical can be modulated by appropriate choice of structure. We can use the approximate McConnell model⁸ relating hyperfine coupling to spin density and assume that the McConnell proportionality constant is (–)22 G, a typical value for delocalized radicals. Using the experimental hfc $a(4) = 1.8$ – 2.1 G in 1 and 2 and $a(2) = 4.2$ and 3.3 G in 3 and 4, the amount of π -spin at these positions is estimated to be 8–10%, 19%, and 15%, respectively.

The experimental estimates of spin density distributions also compare well to the Mulliken spin populations predicted by Gaussian 98 at the 4'-positions for 1 and 2 and the 2'-positions for 3 and 4. Figure 3 summarizes the experimental and computed percent spin density populations for the hfc data in Table 1. The furan ring substituent in the 4-position of the phenoxy radical leads to the largest amount of delocalization, with the thiophene also supporting a large delocalization.

2,4,6-Tri-*tert*-butylphenoxy has a 32% spin density population at the 4-position.⁹ By comparison, 4-phenyl-2,6-di-*tert*-butylphenoxy has no spin density population that is larger than 7% on any *ortho* and *para* position of the 4-phenyl substituent.¹⁰ (The percent spin populations ignore small contributions of negative spin density on some sites.) So, only a modest amount of delocalization occurs from the phenoxy 4-position into the conjugated phenyl ring in 4-phenyl-2,6-di-*tert*-butylphenoxy. By comparison to these phenoxy radicals that lack heteroatom substituents π -conjugated to the 4-position, 1–4 all have spin sites with 10–19% population on the 4-substituent ring. The difference in delocalization is partly attributable to the strong desire of the radicals to place large spin density populations on sites

(5) Duling, D. R. *J. Magn. Reson.* **1994**, *B104*, 105.

(6) Frisch, M. J.; Trucks, G. W.; Schlegel, H. B.; Gill, P. M. W.; Johnson, B. G.; Robb, M. A.; Cheeseman, J. R.; Keith, T.; Petersson, G. A.; Montgomery, J. A.; Raghavachari, K.; Al-Laham, M. A.; Zakrzewski, V. G.; Ortiz, J. V.; Foresman, J. B.; Cioslowski, J.; Stefanov, B. B.; Nanayakkara, A.; Challacombe, M.; Peng, C. Y.; Ayala, P. Y.; Chen, W.; Wong, M. W.; Andres, J. L.; Replogle, E. S.; Gomperts, R.; Martin, R. L.; Fox, D. J.; Binkley, J. S.; Defrees, D. J.; Baker, J.; Stewart, J. P.; Head-Gordon, M.; Gonzalez, C.; Pople, J. A.; Gaussian Inc.: Pittsburgh, PA, 1998.

(7) Xie, C.; Lahti, P. M. *Tetrahedron Lett.* **1999**, *40*, 4305.

(8) $a = Q\rho$, where A is hfc, ρ is π -spin density, and Q is the McConnell constant. See McConnell, H. M. *J. Chem. Phys.* **1956**, *28*, 1188 and Pople, J. A.; Beveridge, D. L. *Approximate Molecular Orbital Theory*; McGraw-Hill: New York, 1970, p 146 ff.

(9) Prabhanada, B. S. *J. Chem. Phys.* **1983**, *79*, 5752.

(10) Mukai, K.; Inagaki, N. *Bull. Chem. Soc. Jpn.* **1980**, *53*, 2695.

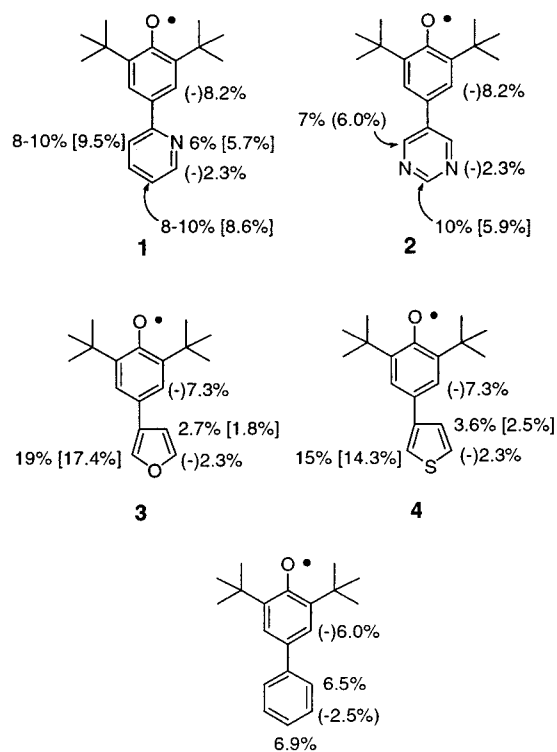


Figure 3. Experimental and [BLYP computed] percent spin populations. Experimental spin densities for 4-phenyl-2,6-di-*tert*-butylphenoxy from ref 9. BLYP computed values were done on model systems with replacement of *tert*-butyl groups by hydrogen atom substituents. Negative (–) spin populations are deduced by spin polarization parity guidelines.

stabilized by adjacent nitrogen, oxygen, or sulfur atoms. There is also an effect of having five-member rings in **3** and **4**, by comparison to a six-membered ring in 4-phenyl-2,6-di-*tert*-butylphenoxy—with one less π -atom, there is more likelihood of a single site with a larger spin population.

Some comparisons to related delocalizable radicals with heteroring substitution are available. 2-Pyridyl-*tert*-butyl nitroxide^{11–12} and 5-pyrimidyl-*tert*-butyl nitroxide are connectivity analogues of **1** and **2**, respectively. The pyridyl compound has previously been generated in trapping experiments, and both have been synthesized by us¹² through metalation of the corresponding bromo compounds, treatment with 2,2-dimethyl-2-nitrosopropane, and oxidation. The nitroxide group is inherently less delocalized than the phenoxy group, but the qualitative spin density patterns in the nitroxides (Scheme 2, experimental hfc given in gauss) are analogous to those in the phenoxy systems.

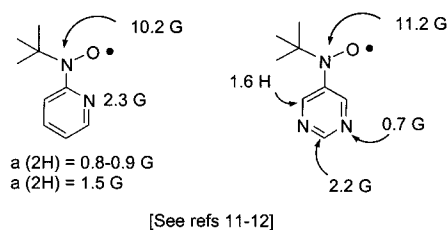
(11) Bentley, T. W.; John, J. A.; Johnstone, R. A. W. *J. Chem. Soc., Perkin Trans. 2* **1973**, 1039–1044.

(12) (a) Lahti, P. M.; Esat, B.; Ferrer, J. R.; Liu, Y.; Marby, K. A.; Xie, C.; George, C.; Antorena, G.; Palacio, F. *Mol. Cryst. Liq. Cryst. Sci. Technol., Sect. A* **1999**, 334, 285–294. (b) Field, L. M.; Marby, K. A.; Lahti, P. M. Unpublished results.

(13) Xie, C.; Lahti, P. M. *J. Polym. Sci. Part A: Polym. Chem.* **1999**, 37, 779.

(14) Yamamoto, T.; Hiyashi, H. *J. Polym. Sci. Part A, Polym. Chem.* **1997**, 35, 463.

Scheme 2



An important consideration in the design of molecular magnetic materials is interaction of spin density in the solid state or in very high spin polymeric materials. The ability to manipulate sites of major spin density by structural variation gives potential electronic control in such materials. For example, our group and Yamamoto's have synthesized 2,5-thienediyl polymers based upon radical **4**.^{13–14} This design was based upon the expectation that delocalization from the pendant phenoxy groups through the polythiophene backbone would be sufficient to allow effective exchange between spin-bearing units. The present results for **4** show that spin delocalization is qualitatively sufficient to meet the original design intent.

This study demonstrates some of the possibilities for modulation of spin density in organic radicals by a “mix-and-match” strategy of attaching heterocyclic systems with π -conjugation to delocalizable radical sites. In particular, the furan and thiophene substituents allow a substantial degree of spin density delocalization away from the phenoxy ring. DFT computations turn out to be very good predictors of the spin density distributions in these systems and should be very useful for prediction of delocalization extents in related phenoxy-based open-shell molecules. Reasonable strategies to incorporate such organic radicals into molecular magnetic materials will combine tuning spin density distribution by this strategy and coordination of sites of higher spin density with paramagnetic ions to strengthen exchange interactions between organic and inorganic units in hybrid material. By these methods we hope to improve the stability and magnetic ordering characteristics of new organic and hybrid organic–inorganic materials.

Acknowledgment. This work was supported by the National Science Foundation (CHE 9809548). The opinions expressed in this paper are solely those of the authors and not necessarily those of the Foundation. We also acknowledge assistance from the Naval Research Laboratory for assistance with crystallographic analysis.

Supporting Information Available: Experimental procedures for syntheses of **1–8**, Gaussian archive files for spin density and hfc computations of **1–4**, tables of crystallographic parameters for **6**, FTIR spectra of **5–8**, **2**, **4**, and **6–CuCl₂**. This material is available via the Internet free of charge from <http://pubs.acs.org>.

OL0063407